# Double-Layer Graphene Optical Modulator

Ming Liu,[†] Xiaobo Yin,[†] and Xiang Zhang*,[†,‡]

[†]NSF Nano-scale Science and Engineering Center (NSEC), 3112 Etcheverry Hall, University of California at Berkeley, Berkeley, California 94720, United States

[‡]Material Sciences Division, Lawrence Berkeley National Laboratory, Berkeley, California 94720, United States

**ABSTRACT:** Here we report a high-performance double-layer graphene optical modulator. By using two graphene layers and an oxide layer in between to form a p-oxide-n like junction, this modulator operates at 1 GHz with a high modulation depth (~0.16 dB/$\mu$m) at a moderate drive voltage (~5 V). Benefited from the symmetrical band structure of graphene near Dirac point, such design eliminates the optical loss widely existing in silicon photonics and has advantages including small footprint, low energy consumption, and low insertion loss.



**KEYWORDS:** Graphene, optical modulator, double layer, optoelectronics
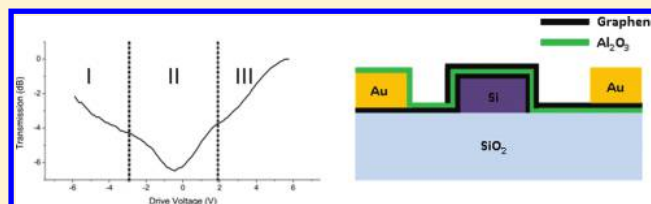
Graphene, a single layer of carbon atoms, has attracted growing attentions due to its outstanding and intriguing properties.[1,2] Possessing the highest carrier mobility of more than 200000 cm$^2$/(V·s), graphene has stirred up particular interest for high-speed electronics and is considered as a promising replacement for silicon for on-chip integration.[3,4] Graphene also shows attractive optical properties over a broad spectral range from the visible to mid-infrared (IR). Graphene-based plasmonic device at the mid-IR regime has been recently explored, and innovative transformation optics has also been proposed on a graphene platform.[5−7] Graphene can absorb 2.3% of the normal incident ultraviolet and visible light even though it has only one atomic layer.[8] This universal absorption coefficient is due to the unique linear and gapless band dispersion of Dirac fermions.[9] Although this absorption is small, novel passive optoelectronics including mode-lock laser, polarizers and photodetectors have already been demonstrated by utilizing the anisotropic absorption property of graphene and the therefore generated hot electrons.[10−13]

Graphene can also be actively tuned in a dramatic way. With the free electrons tightly confined within the single atomic layer, it has a very low density of states, especially when electron energy is close to the Dirac point. Slight variations of carrier density can therefore cause significant shifts in Fermi energy ($E_F$), which changes the rate of interband transitions and subsequently the optical constant.[14] Utilizing this effect, we have recently demonstrated a new type of optical modulator by using graphene as the active medium.[15] In the experiment, a silicon bus waveguide was used as the back gate to dope the graphene sheet, which was placed adjacent to but isolated from the silicon waveguide by an oxide layer. In this approach, ~4 dB modulation depth was achieved on a 40 $\mu$m long silicon waveguide, covering from E to L band in telecommunication. However, by using silicon as the back gate, this structure inherits disadvantages from silicon photonics such as high insertion loss and limited carrier mobilities.

Here we report a design and the first experimental demonstration of a double-layer graphene optical modulator. This design uses a similar structure as a forward/reverse-biased silicon modulator[16] in which the doped silicon is replaced by intrinsic/predoped graphene, removing the insertion loss due to the doped silicon waveguide. Both electrons and holes are injected into graphene layers to form a p-oxide-n like junction, and the optical loss from silicon can be reduced to minimum. This device benefits from the unique linear band dispersion of graphene, which gives a symmetrical DOS near the Dirac point. Because the interband transition coefficient in graphene is only determined by $|E_F|$ but not its sign,[17] both graphene layers can become transparent simultaneously at high drive voltage and the device is thus at "on" state. Such design avoids the participation of electrons/holes in silicon and therefore its operation speed will only be limited by the carrier mobility in graphene. In addition, using two graphene layers for the active medium can further increase the optical absorption and modulation depth, giving advantages including smaller footprint and lower power consumptions.

Figure 1 illustrates our approach to fabricate the double-layer graphene optical modulator. The fabrication starts with commercial silicon-on-insulator (SOI) wafers with a device layer thickness of 340 nm and a buried-oxide thickness of 2 $\mu$m. A 400 nm wide silicon waveguide with both ends connected to a pair of grating couplers (period = 780 nm, optimized for $\lambda$ = 1537 nm) were fabricated using deep reactive-ion etch (DRIE). Atomic layer deposition (ALD) technique was then employed to conformally coat a 5 nm thick Al$_2$O$_3$ isolation layer to prevent potential carrier injections from the bottom graphene layer into the silicon. Chip-sized graphene sheet, prepared on Cu film by CVD method,[18] was first protected by 200 nm thick
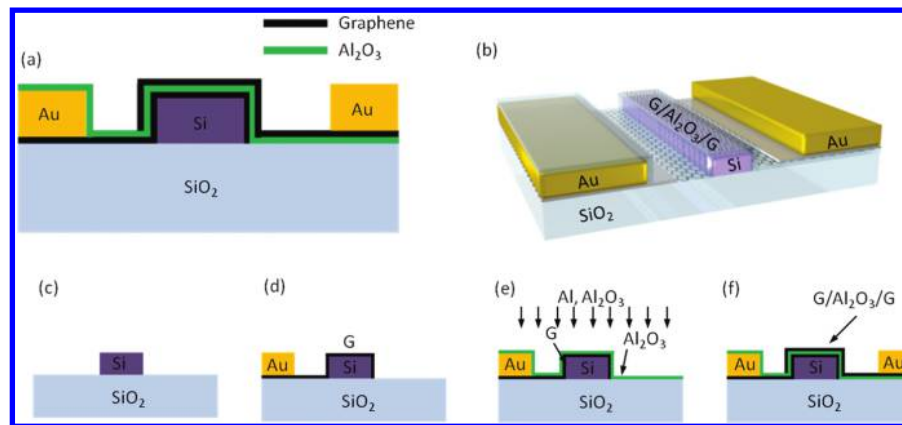
**Figure 1.** Schematic illustration of the fabrication process for the double layer graphene modulator. (a,b) The final structure of the device. The fabrication starts from the silicon waveguide prepared from a SOI wafer, as shown in (c). In (d), mechanical transfer of CVD prepared graphene sheet. Use of e-beam lithography (EBL) and oxygen plasma to remove unwanted region and then deposit of electrode. (e) Deposit of thin layer of Al by thermal evaporation, then deposit of $Al_2O_3$ by ALD. (f) Mechanical transfer of the second graphene sheet. Use of EBL and oxygen plasma to define the active region. Deposit of metal for electrode.

poly(methyl methacrylate) (PMMA) film which was baked at 110 °C for 10 min. After the Cu film was removed by $FeCl_3$ solution (45%, Sigma-Aldrich), the graphene sheet was then rinsed and transferred on the waveguides for overnight baking. E-beam lithography was then used to define the active region, and oxygen plasma was applied to remove undesired graphene on one side of the waveguide, leaving the other side for metallization (Pd/Au, 10/100 nm).

Direct deposition of high dielectric constant material through ALD growth on pristine graphene is challenging, owing to the hydrophobic nature of graphene basal plane.[19,20] We instead deposited 1 nm of aluminum, which was immediately oxidized into $Al_2O_3$ upon exposure to the air, onto the bottom graphene layer for the following ALD deposition (Figure 1e). Using the oxidized aluminum as seed, 12 nm of $Al_2O_3$ was then conformally deposited at 200 °C. The top graphene layer was then mechanically transferred onto the dies forming the desired capacitor structures. Subsequently, similar patterning and etching procedures as the bottom graphene layer were performed to define the active tuning areas of graphene and top metal electrodes. Shown in Figure 1f is the cross-section view of the device that is ready for measurement.

The static optical transmission of the device was measured at the wavelength of 1537 nm, under different drive voltages. The peak transmission of the system was found to be $3 \times 10^{-3}$ (or −25 dB) with most of the insertion loss coming from the grating couplers (~14.6 dB for two couplers). As shown in Figure 2, 6.5 dB modulation depth was achieved on a 40 $\mu$m long device with HE mode excited, leaving ~4 dB insertion loss from graphene. Since the optical loss induced by intraband electron transition is of orders smaller than interband transition,[17] this insertion loss is due to the impurities or nonuniform charge distributions on graphene. The switching voltage of about 6 V for this device was only determined by the dielectric constant and thickness of the gate oxide, and the leak current was at the order of nanoamperes. This modulation depth, as expected, is almost two times of the single layer graphene modulator.[15] Another prominent feature is that the modulation curve is more symmetrical, arising from the structural symmetry of the top and bottom graphene layers. Three regions can be clearly differentiated from the curve, and each of them corresponds to a band structure model given in
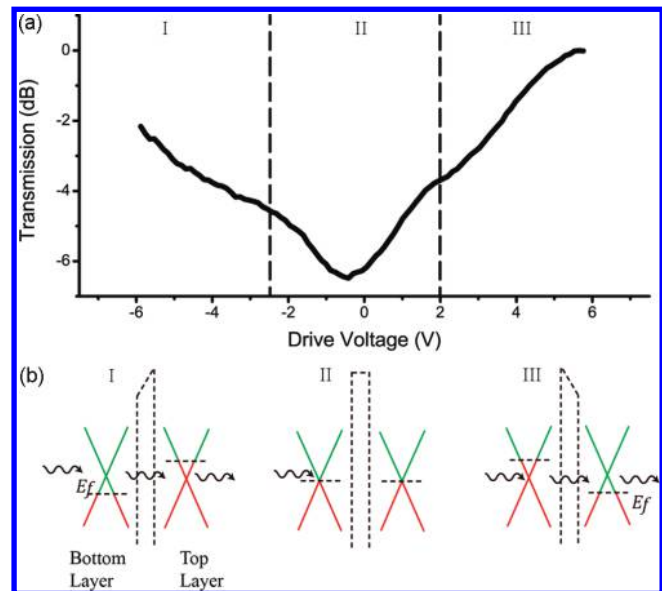


**Figure 2.** Static response of a double layer graphene modulator. Modulation depth of ~6.5 dB can be achieved on a 40 $\mu$m long device at the wavelength 1.537 $\mu$m. (b) The graphene band profiles (green for unoccupied state, red for occupied states) for regions I, II, and III in (a). The arrows represent the incident photons.

Figure 2b. When the drive voltage is close to zero, both graphene layers are undoped, or only slightly doped due to the environment. Therefore Fermi levels are close to the Dirac point, and both graphene sheets are absorptive to light (evanescent wave in this case). When the voltage is added between them, two graphene layers form a simple parallel capacitor model with one graphene layer doped by holes and the other by electrons at the same doping level. Linear energy dispersion in graphene band structure gives a Fermi level shift of $\Delta E_F = \hbar v_F (\pi |n|)^{1/2}$, where $\hbar$ is the Plank constant divided by $2\pi$, $v_F$ is the Fermi velocity, and $n$ is the electron/hold doping concentration. When the Fermi level shift in both graphene layers reach half photon energy of incident light, both graphene layers become transparent simultaneously. Changing the sign of the drive voltage only switches the roles of graphene layers as anode and cathode and gives similar response to the incident

light. The lowest transmission point was shifted from zero due to the predoping (total $2 \times 10^{12}$ cm$^{-2}$) on graphene layers. The asymmetry of the transmission curve was owing to the different environments for the top and bottom graphene layers, as the top one has only one side contact with $Al_2O_3$ while the bottom layer was sandwiched between two $Al_2O_3$ layers.[21]

To measure the dynamic response of the modulator, electrical signal generated by a network analyzer (Agilent, E5071C) was superimposed onto a static drive voltage for small signal measurement. Figure 3 shows the dynamic response of
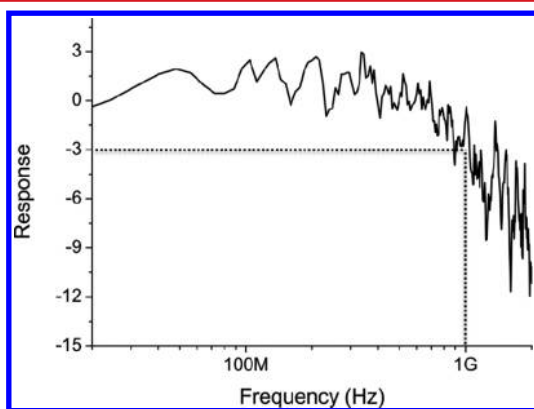


**Figure 3.** Dynamic response of the device. The 3 dB bandwidth is found to be ~1 GHz.

the device in the frequency range from 20 M to 2 GHz. The 3 dB cutoff of the device is at about 1 GHz with static drive voltage of 2 V. Further analysis from S11 shows that the capacitance of the device was about 0.1 pF, which agrees well with a simple parallel-capacitance model. Since the drive voltage is ~5 V and the leak current is negligible, the power consumption is at the level of 1 pJ/bit. S11 analysis also reveals that the high series resistance (~1kΩ) is the major reason for the low operation speed. Since the low graphene sheet resistant (~200 Ω/□ when far away from Dirac point) contributes only ~10 Ω to the total resistance if we consider the graphene as a 40 $\mu$m long 2 $\mu$m wide stripe, the high series resistance is mainly contributed from the contact resistance between graphene layer and palladium electrode. Improvements in the metal–graphene contact, such as plasma treatment, will not influence the insertion loss of the device, since the electrodes are 600 nm away from the active region and do not affect the optical mode. By reducing the series resistance to the level of 10−100 Ω, a much higher 3 dB bandwidth can be expected.

To optimize the modulation depth of the device, different waveguide width was numerically analyzed by using finite element analysis. The active region is assumed to include both the top and sidewalls of the waveguide. In practice, the mechanically transferred graphene may not closely contact all sidewalls. However, this shall not change significantly the overall absorption as the evanescent field of the waveguide mode spreads about a hundred of nanometers away from the waveguide sidewalls. Refractive index of undoped graphene is derived from the optical conductivity of graphene.[5] Figure 4 shows the decay length of the light versus different waveguide width. With a wide waveguide, the HE mode gives better modulation ability (shorter decay length) than the EH mode. This is because the overall tangential electrical field integrated on the top surface in the HE mode is greater than that in the
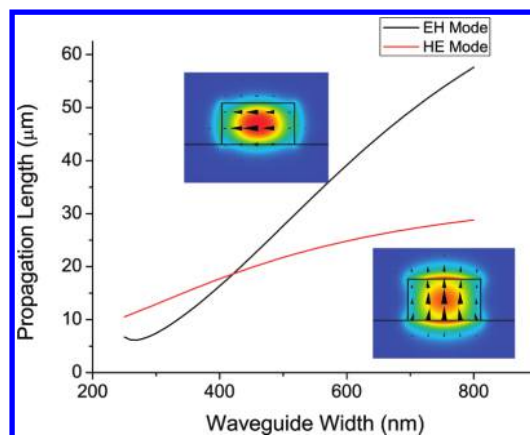


**Figure 4.** Propagation length of the device under different waveguide widths. Electric field distributions of two typical modes, EH and HE, are plotted in the insets. Black arrows show the directions of electric fields. Double layer graphene layers coat both the top surface and sidewalls of the waveguide.

EH mode. It also indicates that narrower waveguide, which has higher surface-volume ratio, will give better performance.

In conclusion, we have designed and experimentally demonstrated the first double-layer graphene modulator at high modulation depth (~0.16 dB/$\mu$m). By using two graphene layers to form a p-oxide-n like junction, such design avoids the insertion loss from doped silicon and can potentially work at high frequency. It can be easily expanded to include multipairs of double graphene layers, which can leads to further device improvements such as smaller device footprint and lower energy consumption.

## ■ AUTHOR INFORMATION

### Corresponding Author
*E-mail: xiang@berkeley.edu.

### Notes
The authors declare no competing financial interest.

## ■ REFERENCES

(1) Geim, A. K.; Novoselov, K. S. *Nat. Mater.* **2007**, *6* (3), 183−191.
(2) Bonaccorso, F.; Sun, Z.; Hasan, T.; Ferrari, A. *Nat. Photonics* **2010**, *4*, 611.
(3) Bolotin, K. I.; Sikes, K. J.; Jiang, Z.; Klima, M.; Fudenberg, G.; Hone, J.; Kim, P.; Stormer, H. L. *Solid State Commun.* **2008**, *146* (9−10), 351−355.
(4) Avouris, P.; Chen, Z. H.; Perebeinos, V. *Nat. Nanotechnol.* **2007**, *2* (10), 605−615.
(5) Vakil, A.; Engheta, N. *Science* **2011**, *332* (6035), 1291−1294.
(6) Ju, L.; Geng, B. S.; Horng, J.; Girit, C.; Martin, M.; Hao, Z.; Bechtel, H. A.; Liang, X. G.; Zettl, A.; Shen, Y. R.; Wang, F. *Nat. Nanotechnol.* **2011**, *6* (10), 630−634.
(7) Chen, P. Y.; Alu, A. *ACS Nano* **2011**, *5* (7), 5855−5863.
(8) Mak, K. F.; Sfeir, M. Y.; Wu, Y.; Lui, C. H.; Misewich, J. A.; Heinz, T. F. *Phys. Rev. Lett.* **2008**, *101* (19), 196405.
(9) Zhou, S. Y.; Gweon, G. H.; Graf, J.; Fedorov, A. V.; Spataru, C. D.; Diehl, R. D.; Kopelevich, Y.; Lee, D. H.; Louie, S. G.; Lanzara, A. *Nat. Phys.* **2006**, *2* (9), 595−599.

(10) Sun, Z. P.; Popa, D.; Hasan, T.; Torrisi, F.; Wang, F. Q.; Kelleher, E. J. R.; Travers, J. C.; Nicolosi, V.; Ferrari, A. C. *Nano Res.* **2010**, *3* (9), 653−660.

(11) Bao, Q. L.; Zhang, H.; Wang, B.; Ni, Z. H.; Lim, C. H. Y. X.; Wang, Y.; Tang, D. Y.; Loh, K. P. *Nat. Photonics* **2011**, *5* (7), 411−415.

(12) Xia, F. N.; Mueller, T.; Lin, Y. M.; Valdes-Garcia, A.; Avouris, P. *Nat. Nanotechnol.* **2009**, *4* (12), 839−843.

(13) Mueller, T.; Xia, F. N. A.; Avouris, P. *Nat. Photonics* **2010**, *4* (5), 297−301.

(14) Wang, F.; Zhang, Y.; Tian, C.; Girit, C.; Zettl, A.; Crommie, M.; Shen, Y. R. *Science* **2008**, *320* (5873), 206−209.

(15) Liu, M.; Yin, X. B.; Ulin-Avila, E.; Geng, B. S.; Zentgraf, T.; Ju, L.; Wang, F.; Zhang, X. *Nature* **2011**, *474* (7349), 64−67.

(16) Reed, G. T.; Mashanovich, G.; Gardes, F. Y.; Thomson, D. J. *Nat. Photonics* **2010**, *4* (8), 518−526.

(17) Hanson, G. W. *J. Appl. Phys.* **2008**, *103* (6), 064302.

(18) Li, X.; Cai, W.; An, J.; Kim, S.; Nah, J.; Yang, D.; Piner, R.; Velamakanni, A.; Jung, I.; Tutuc, E.; Banerjee, S. K.; Colombo, L.; Ruoff, R. S. *Science* **2009**, *324* (5932), 1312−1314.

(19) Hollander, M. J.; LaBella, M.; Hughes, Z. R.; Zhu, M.; Trumbull, K. A.; Cavalero, R.; Snyder, D. W.; Wang, X. J.; Hwang, E.; Datta, S.; Robinson, J. A. *Nano Lett.* **2011**, *11* (9), 3601−3607.

(20) Kim, S.; Nah, J.; Jo, I.; Shahrjerdi, D.; Colombo, L.; Yao, Z.; Tutuc, E.; Banerjee, S. K. *Appl. Phys. Lett.* **2009**, *94* (6), 062107.

(21) Joshi, P.; Romero, H. E.; Neal, A. T.; Toutam, V. K.; Tadigadapa, S. A. *J. Phys.: Condens. Matter* **2010**, *22* (33), 334214 .